JOURNAL OF MATERIALS SCIENCE 12 (1977) 1209–1214

The macroscopic yielding behaviour of polymers in multiaxial stress fields

K. D. PAE
High Pressure Research Laboratory and Department of Mechanics and Materials Science, Rutgers University, New Brunswick, New Jersey, USA

Experimental data on yielding of polyoxymethylene (POM) and polypropylene (PP) have been obtained in a wide range of complex triaxial stress conditions. These complex triaxial stress states have been produced by superimposition of simple stresses such as uniaxial compression, uniaxial tension and pure shear on hydrostatic pressure of various intensities. The actual yield surfaces of both polymers were constructed using the data. The yield surface of POM is a cone-shaped with a pointed apex and straight edges, while the yield surface of PP is cone-lime and non-linear, also with a pointed apex. A yield criterion is shown to very closely predict the observed behaviour of both polymers.

1. Introduction

Polymeric materials in general respond in a quite different manner to different loading conditions. Even simple states of applied stress such as tension, compression and pure shear produce vastly different responses in yielding, deformation, and fracture behaviours. When the state of stress is complex, these behaviours undergo dramatic changes, and equally dramatic changes in these responses occur from one polymer to another [1].

Many investigators have studied yielding behaviour of polymers in uniaxial stress conditions, biaxial stress conditions and, more recently, triaxial stress conditions [2–9]. However, the range of state of stress covered on each of these studies was limited to a narrow region in view of the entire yield surface, and thus it has not been possible to construct the entire yield surface of any polymers, crystalline or amorphous. These investigators have also speculated on the possible shape of yield surfaces.

This paper presents experimental data on polyoxymethylene (POM) and polypropylene (PP) in a wide range of stress conditions, and shows for the first time the construction of actual yield surface using the data. A yield theory proposed earlier [10] is shown to very closely predict the observed behaviour of both polymers.

2. Materials and experimental

The materials used in the study were obtained from a commercial source. The density of POM (du Pont Delrin 500) was 1.425 g cm^{-3} and that of PP was 0.905 g cm^{-3}. Samples were machined, taking care not to heat the samples during machining, to the forms of straight circular cylinders for compression tests, circular cylinders with threaded raised ends for tension tests, and circular hollow cylinders with raised but square ends for torsion tests.

The experimental study involves testing the samples in different triaxial stress conditions. A method of producing controlled but complex triaxial stress conditions is superimposition of simple stresses such as uniaxial compression, uniaxial tension, and pure shear on hydrostatic pressure of various intensities.

A new electromechanical testing apparatus has been constructed for carrying out torsional tests in a hydrostatic pressure environment, and detailed description of the apparatus will be published elsewhere.

The apparatus, which is capable of containing pressures up to 7 kbar, consists of two interconnected thick-walled cylinders, one for testing and the other for pressure compensation. The applied torque is measured by a full-bridge strain gauge

TABLE I Experimental and predicted values of yield stresses at various pressures for polyoxymethylene

Hydrostatic pressure		Average experimental yield stresses (psi) × 10^{-3}			Predicted yield stress (psi) × 10^{-3}		
(psi) × 10^3	(kbar)	Compression	Tension	Shear	Compression	Tension	Shear
Atm.	Atm.	11.2	10.6	7.3	13.1	12.1	7.3
10	0.69		13.3			13.2	
14.5	1.00			8.4			8.3
20	1.38	15.1	14.9		15.6	14.4	
29	2.00			9.7			9.3
30	2.07		16.0			15.5	
40	2.76	18.1	16.8		18.6	16.7	
43.5	3.00		10.5				10.3
58	4.00			11.3			11.3
60	4.13	20.0	19.1		20.5	19.0	
72.5	5.00			12.3			12.3
80	5.52	23.0	22.8		23.0	21.3	
87	6.00			13.9			13.3
100	5.90	25.9	23.6		25.5	23.6	

1 kbar = 14 500 psi = 980.7 kg cm^{-2}.

which is mounted within the torque shaft, unexposed to the pressure medium and unaffected by the friction in the seals. The rotational displacement of the specimen is detected internally by a contact point moving on a toothed wheel and externally by a rotary variable differential transformer. A torsional specimen was completely immersed in a hydro-static pressure environment and torsional shear stress was then superimposed. The apparatus for carrying out compression and tension tests has been in existence for quite some time [11]. Testing speeds were 0.0017 in sec^{-1} for compression and tension, and 0.020 rad sec^{-1} for torsion which are equivalent to a normal strain-rate of about 0.002 sec^{-1} and a shear strain-rate of about 0.008 sec^{-1}; therefore the tests were assumed to be quasi-static. The possible differences in the yield stresses due to the differences in strain-rates at these rates were certainly small and were well within experimental error. In addition, the time effect was neglected in analysing the data. The pressure medium used was a mixture of kerosene and a small amount of a lubricant oil. The medium was found to have no effect on the yielding of POM and PP.

3. Results and discussion

Load–deformation curves for compression and tension tests, and torque-angular rotation curves for torsional shear tests have been obtained at various pressures up to 7 kbar and then were converted to stress–strain diagrams. From the stress–strain diagrams, the values of yield strengths were determined by an offset method (2%). The yield stress values in compression, tension, and shear are given in Table I for POM and in Table II for PP, together with predicted values. Each value in the table is an average of a minimum of three and often eight tests. Figs. 1 and 2 show the yield stresses in compression, tension and shear, plotted against hydrostatic pressure for POM and PP, respectively. Each experimental point represents the average values. The solid lines in the figures are the theoretical prediction by a yield criterion to be

TABLE II Experimental and predicted values of yield stresses at various pressures for polypropylene

Hydrostatic pressure		Average experimental yield stresses (psi) × 10^{-3}			Predicted yield stress (psi) × 10^{-3}		
(psi) × 10^{-3}	(kbar)	Compression	Tension	Shear	Compression	Tension	Shear
Atm.	atm.	6.6	5.4	3.5	6.6	5.4	3.4
14.5	1.00	10.8	8.9	5.8	11.0	9.2	5.8
29	2.00	16.5	14.4	8.3	15.1	12.8	8.0
43.5	3.00	19.5	17.0	10.6	18.8	16.1	10.0
58	4.00	22.5	19.6	11.7	22.0	19.2	11.9
72.5	5.00	25.5	23.2	12.7	25.0	22.4	13.5
87	6.00	27.5	25.6	13.8	27.5	24.6	15.0
101.5	7.00	29.0	26.7		29.8	27.0	16.4

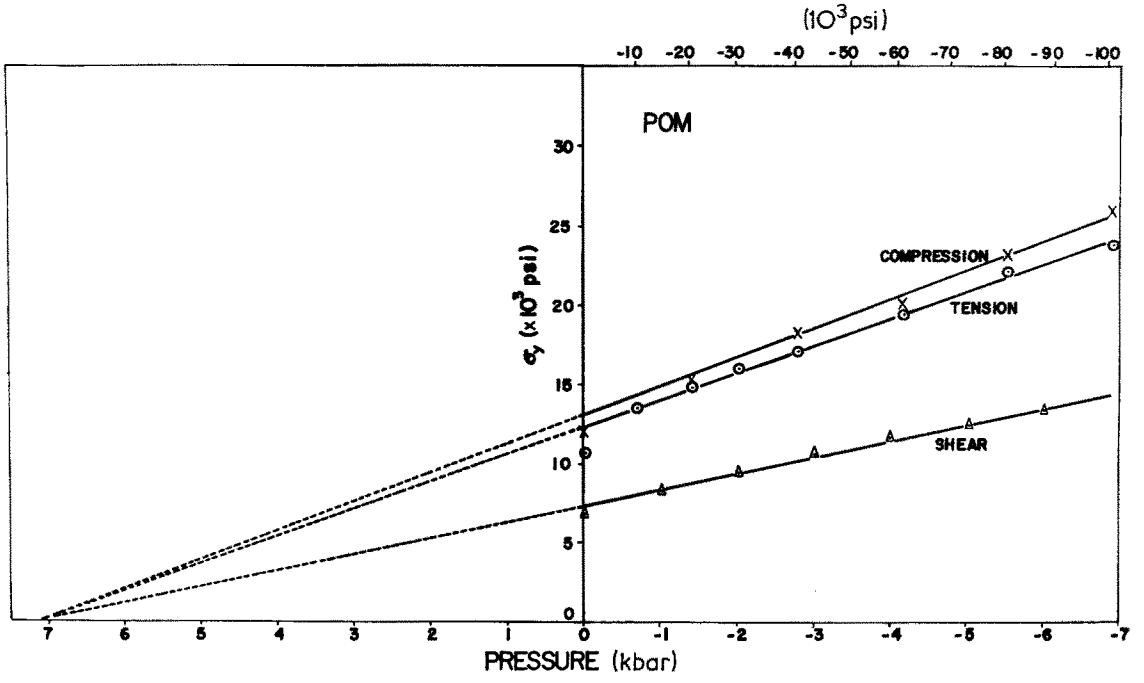

Figure 1 Yield stresses versus hydrostatic stress for polyoxymethylene.

discussed later in this section.

For POM, each of the yield stresses in compression, tension, and shear was found to be an increasing linear function of hydrostatic pressure, except the yield stress values at atmospheric pressure which were slightly off linearity. The compressive yield stress was consistently greatest at a given pressure and increased at the highest rate with increasing pressure. The shear yield stress, on the other hand, was the lowest in the value at a given pressure, and also increased at the lowest rate. The tensile yield stress and the rate of increase both lie between the values of compression and shear. It is significant that when all data points for each yield stress are extrapolated in the direction of hydrostatic tension, all three converge on a

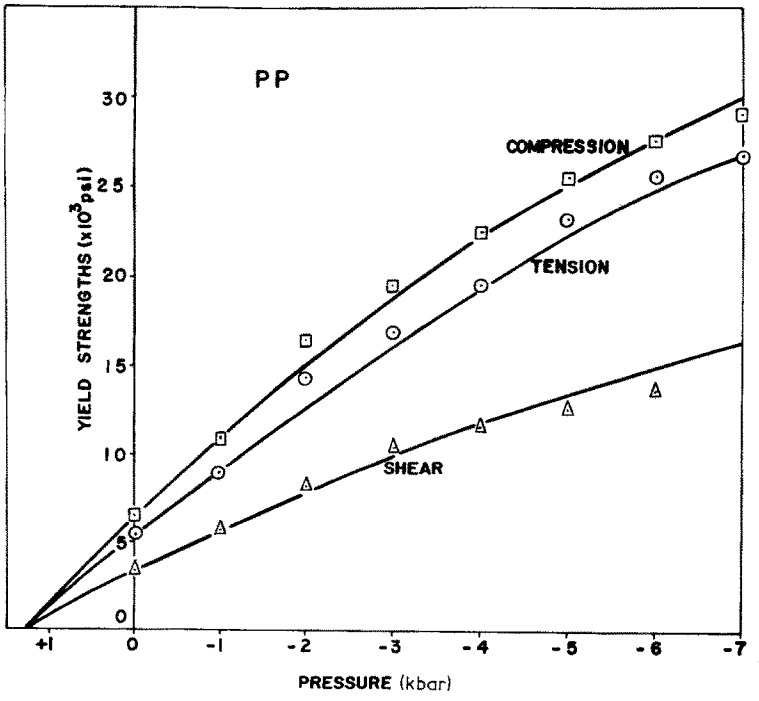

Figure 2 Yield stresses versus hydrostatic stress for polypropylene.

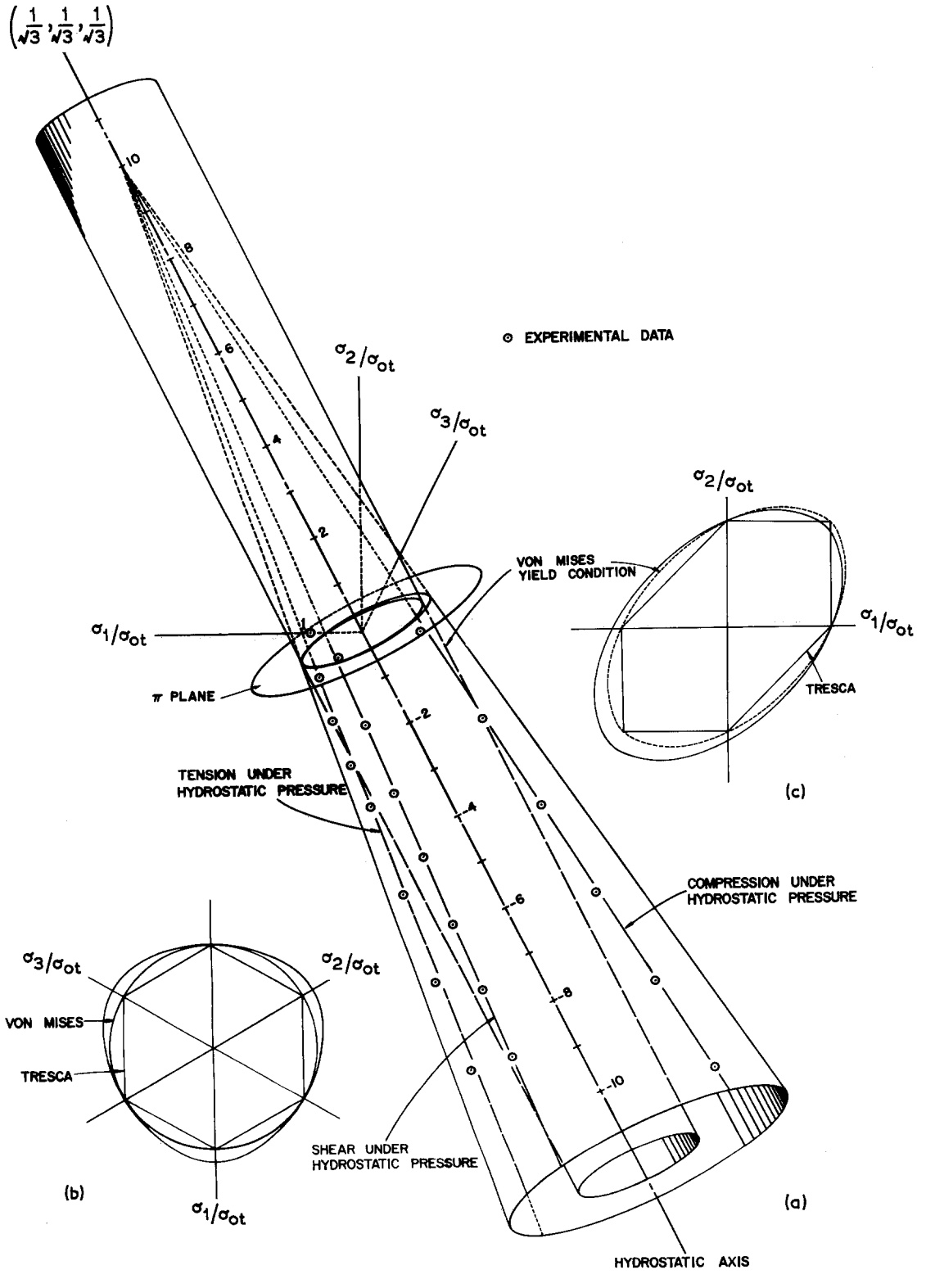

Figure 3(a) Yield surface of polyoxymethylene. (b) Intersection of the surface with the π-plane. (c) Two-dimensional projection of the surface at atmospheric pressure.

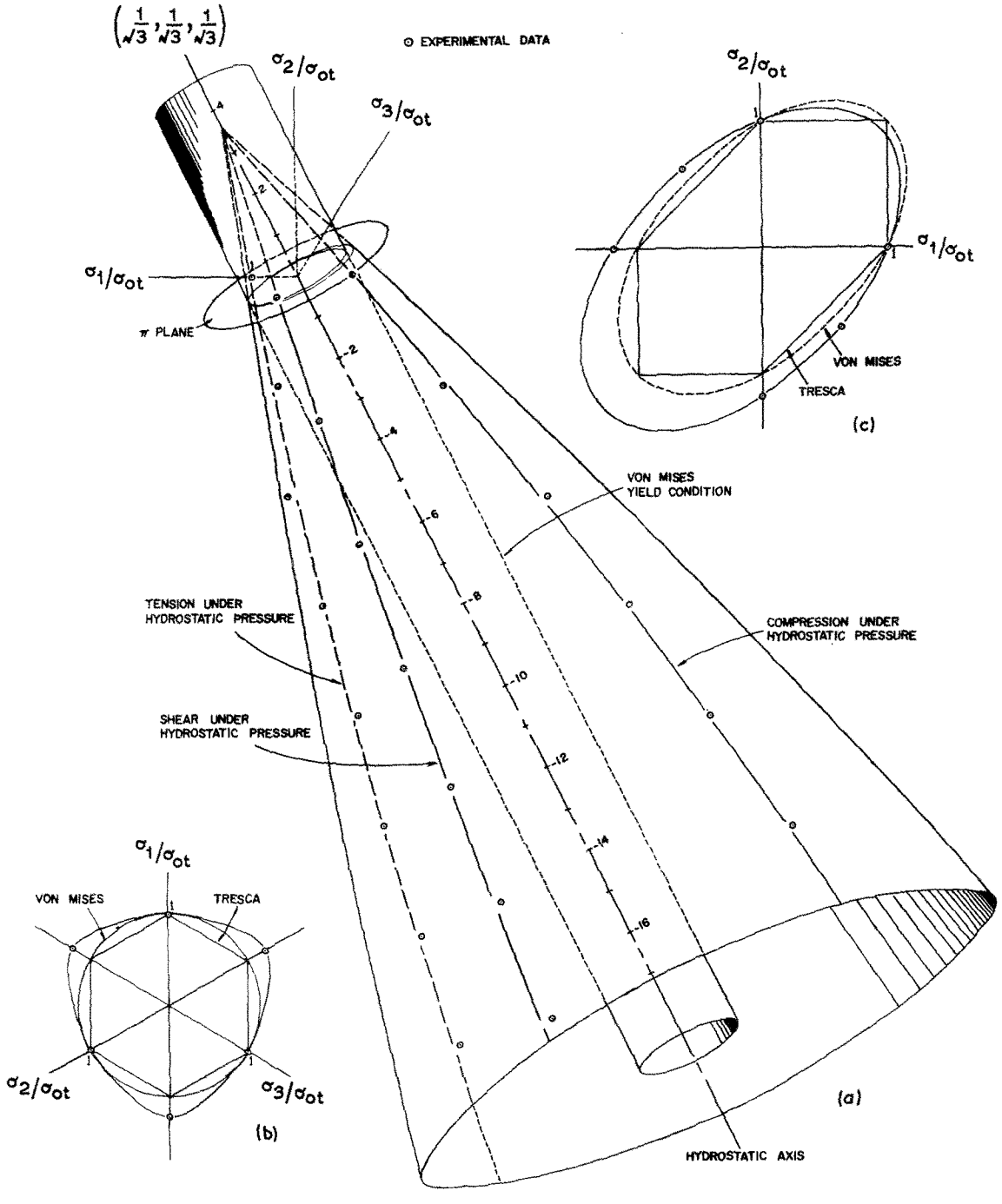

Figure 4(a) Yield surface of polypropylene. (b) Intersection of the surface with the π-plane. (c) Two-dimensional projection of the surface at atmospheric pressure.

point at $p = +7.3$ kbar. This means that POM, if also subjected to hydrostatic tension, will yield under compression, tension and shear with less stress than at atmospheric pressure as can be seen from Fig. 1. This is exactly the opposite effect that is produced when hydrostatic pressure is superimposed on the simple stresses. Furthermore, more importantly, this also indicates that POM will yield under triaxial tensile stresses of equal magnitude alone. The magnitude of hydrostatic tensile stress for POM was determined, to be $p = +7.3$ kbar, by extrapolation of the experimental data, as shown in Fig. 1.

When the results of Fig. 1 are replotted they

form a cone with a pointed apex and straight edges, as shown in Fig. 3a. The small circles are the experimental data and the lines represent the theoretical prediction. Fig. 3b shows the intersection of the surface at zero (or atmospheric) pressure with the π-plane, i.e. a hyperplane whose normal is in the direction of the hydrostatic axiz ($1/\sqrt{3}$, $1/\sqrt{3}$, $1/\sqrt{3}$) located at zero pressure). This represents the cross-sectional shape of the surface. Von Mises' and Tresca's projections are shown together here for comparison purposes. Fig. 3c shows the two-dimensional projection of the surface at zero pressure.

For PP, the dependence of all three yield stresses on hydrostatic pressure is non-linear, with compressive yield stress always being greatest, tensile yield stress the second greatest, and shear yield stress the lowest. When all data are extrapolated in the direction of the hydrostatic tensile axis, all three curves again meet at a point $p = +1.35$ kbar. In other words, PP yields with a decreased stress under compression, tension, and shear when subjected to a hydrostatic tensile field, as opposed to an increased stressunder a hydrostatic pressure field. In addition, PP will yield under triaxial tensile stress of equal magnitude, $p = 1.35$ kbar. When the results of Fig. 2 are replotted they give a non-linear cone with a pointed apex, as shown in Fig. 4a. Again, the small circles represent the experimental data, and the solid line represents the theoretical prediction. Fig. 4b shows the intersection of the surface at atmospheric pressure with the π-plane, and Fig. 4c, the $\sigma_1 - \sigma_2$ plane projection of the surface at zero pressure. Again, Fig. 4b is the cross-sectional shape of the surface perpendicular to the hydrostatic axis.

The yield condition [10] which predicts the yielding behaviour is of the form

$$(J_2')^{1/2} = \sum_{i=0}^{N} \alpha_i (J_1)^i \qquad (1)$$

where

$$J_2' = \tfrac{1}{6}[(\sigma_1 - \sigma_2)^2 + (\sigma_2 - \sigma_3)^2 + (\sigma_3 - \sigma_1)^2]$$
$$= \tfrac{1}{6}[(\sigma_x - \sigma_y)^2 + (\sigma_y - \sigma_z)^2 + (\sigma_z - \sigma_x)^2] + \tau_{xy}^2 + \tau_{yz}^2 + \tau_{zx}^2$$

is the second invariant of the deviatoric stress tensor,

$$J_1 = \sigma_1 + \sigma_2 + \sigma_3 = \sigma_x + \sigma_y + \sigma_z$$

is the first invarient of stress tensor, and α_i material constants.

Equation 1 may be reduced to various forms depending on the value of N. If $N = 0$, it reduces to von Mises' yield criterion

$$J_2' = \alpha_0^2 = k^2. \qquad (2)$$

If $N = 1$,

$$(J_2')^{1/2} = \alpha_0 + \alpha_1 J_1 \qquad (3)$$

and if $N = 2$,

$$(J_2')^{1/2} = \alpha_0 + \alpha_1 J_1 + \alpha_2 J_1^2. \qquad (4)$$

Equation 3 is used for predicting the yield behaviour of POM, while Equation 4 is used for PP. The material constants in Equations 3 and 4 are determined and tablulated in Table III. Equations 3 and 4, with the appropriate material constants from Table III, can be used for any combinations of stresses from simple stress to multiaxial complex stress.

TABLE III

Material	α_0	α_1	α_2
POM	7.25×10^3	−0.0230	
PP	3.43×10^3	− .0564	$-.0456 \times 10^{-6}$

It should be noted that the yield criterion, Equation 1, among many others [2, 5, 6, 12] is the only criterion which can predict the yield behaviour of both POM and PP.

Acknowledgement

The financial support for this work by National Science Foundation (Grant No. DMR73-0752A02) is gratefully acknowledged.

References

1. K. D. PAE and S. K. BHATEJA, *J. Macromol. Sci.-Rev. Macromol. Chem.* C13 (1975) 1.
2. W. WHITNEY and R. D. ANDREWS, *J. Polymer Sci.* C16 (1967) 2981.
3. A. S. ARGON, R. D. ANDREWS, J. A. GODRICK and W. WHITNEY, *J. Appl. Phys.* 39 (1968) 1899.
4. J. C. BAUWENS, *J. Polymer Sci. A–2* 8 (1970) 893.
5. S. S. STERNSTEIN and F. A. MYERS, *J. Macromol. Sci.-Phys.* B8 (1973) 539.
6. R. M. CADDELL, R. S. RAGHAVA and A. G. ATKINS, *Mater. Sci. Eng.* 13 (1974) 113.
7. S. RABINOWITZ, I. M. WARD and J. S. C. PARRY, *ibid* 5 (1970) 29.
8. A. W. CHRISTIANSEN, E. BAER and S. V. RADCLIFFE, *Phil. Mag.* 24 (1971) 451.
9. J. C. M. LI and J. B. C. WU, *J. Mater. Sci.* 11 (1976) 445.
10. A. A. SILANO, S. K. BHATEJA and K. D. PAE, Intern. *J. Polymeric Mat.* 3 (1974) 117.
11. J. A. SAUER, D. R. MEARS and K. D. PAE, *Europ. Polymer J.* 6 (1970) 1015.
12. A. NADAI "Theory of Flow and Fracture of Solids" (McGraw-Hill, New York, 1950).

Received 25 August and accepted 5 November 1976.